Design and novel turn-off mechanism in transistor lasers

IOP Publishing J. Phys. Photonics 3 (2021) 034018 https://doi.org/10.1088/2515-7647/ac0b4d

Journal of Physics: Photonics

OPEN ACCESS

RECEIVED
29 December 2020

REVISED
19 May 2021

ACCEPTED FOR PUBLICATION
15 June 2021

PUBLISHED
2 July 2021

PAPER

Design and novel turn-off mechanism in transistor lasers

Bohao Wu, John M Dallesasse and Jean-Pierre Leburton*

Department of Electrical and Computer Engineering and N Holonyak Jr Micro and Nanotechnology Laboratory, University of Illinois at Urbana-Champaign, Urbana, IL 61801, United States of America

* Author to whom any correspondence should be addressed.

E-mail: jleburto@illinois.edu

Keywords: three-terminal photonics, speed response, tunneling, computational modeling

Abstract

We provide a quantitative analysis of the spontaneous recombination time in the quantum well (QW) of a transistor laser (TL) that shows that owing to the heavy doping in the base of the transistor, Auger recombination is responsible for the short carrier lifetime and low quantum efficiency of the device. By taking advantage of the QW location close to the collector in the TL three-terminal configuration, we devise a new turn-off mechanism that results in quick electron tunneling through the QW barrier by applying a high base-collector reverse bias to deplete the QW and suppress further recombination. For practical base-collector reverse bias, tunneling time from the QW is on the order of 10th of picosecond, which with a lighter base doping density would simultaneously achieve a fast TL turn-off response, while reducing Auger recombination.

1. Introduction

The transistor laser (TL), invented in 2004 [1], has drawn significant attention both in experimental [2–7] and theoretical [8–16] applications because of its potential application in high-speed optical integration. A typical light-emitting transistor is a three-port heterojunction n–p–n bipolar device featuring a heavily p-doped GaAs base region that contains one or several InGaAs quantum wells (QWs) [5]. Unlike two-port laser diodes, injected electrons in the TL base do not dwell within the active lasing region before recombining but instead sweep quickly from the emitter to the collector across the narrow base with some captured by the QW before recombining. The fast nature of electron transport combined with the abundance of holes in the QW(s) make the TL a promising candidate as a high-speed light-emitter. Indeed, experimental data on the TL frequency response suggests carrier lifetime in the QW ranging from 6.5 to 100 ps [4], which is very fast. However, the high p-doping density up to $4 \times 10^{19}\text{cm}^{-3}$ in the base casts doubt on the radiative nature of carrier recombination in the QW(s). In fact, recent theoretical work confirms this view by claiming that in the heavily p-doped TL base, space charge effects caused by the spatial separation between the ionized acceptors and the dense presence of holes in modulation doped QWs result in a band bending that relaxes carrier confinement in the valence band (VB) [15]. This effect delocalizes the quantum states that spread into the base, and reduces the dipole matrix element (overlap) between conduction band (CB) and VB states so that radiative carrier lifetime barely reaches sub-nanosecond time scale, suggesting other mechanisms dominate the recombination process [15]. This observation is important because the weakness of radiative recombination drastically affects the device quantum efficiency, which is directly related to the TL power performance. Past experimental results indicated that incremental lasing output power of 200 μW requires an additional base current of 40 mA in early TL [6]. As the wavelength of the QW emitted light was 980 nm, the quantum efficiency of this device was only 0.5%. More recent TL data have shown a considerable improvement in the optical power response of 1 mW per 10 mA base current increment, resulting in a quantum efficiency of 10% [7], which is still far below traditional diode laser performance [17]. It is therefore imperative to identify the cause of these poor performances, and remedy it by proposing a new TL design.

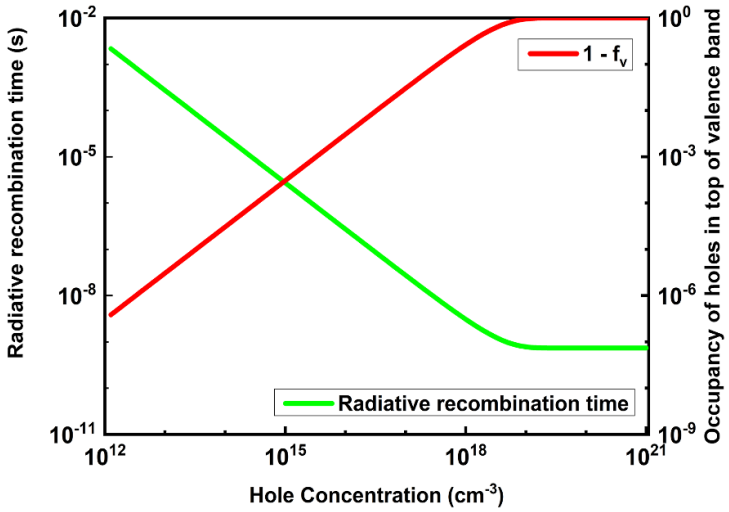

Figure 1. Spontaneous recombination time and occupancy of holes as functions of doping concentration. From first principles, these two terms are inverse-proportional.

2. Origin of the short carrier lifetime in current TL operation

In order to assess the magnitude of the radiative lifetime of the carrier in the InGaAs QW, we compute the radiative recombination rate r_{d} (in $\mathrm{s}^{-1}\,\mathrm{cm}^{-2}$) from first principles [18]:

$$r_{\mathrm{d}}\left(E=\hbar\omega\right)=\frac{2\pi}{\hbar}\left(\frac{eA_0}{2m_0}\right)^2\left|\langle\hat{e}_0\cdot P_{\mathrm{cv}}\rangle\right|^2\times\frac{2}{A}\sum_{n,m}I_{\mathrm{hm}}^{\mathrm{en}}\sum_{\vec{k},\vec{k}'}\delta_{\vec{k},\vec{k}'}\delta\left(K_{\mathrm{c}}+E_{\mathrm{cn}}-K_{\mathrm{v}}'-E_{\mathrm{vm}}-\hbar\omega\right)f_{\mathrm{c}}\left(1-f_{\mathrm{v}}\right). \quad (1)$$

Here e is the elementary charge, A_0 is the absolute value of the vector potential, m_0 is the free electron mass, $\hat{e}_0$ is a unit vector of the optical electric field polarization, P_{cv} is the momentum matrix element between the initial atomic state $|c\rangle$ and the final atomic state $|v\rangle$, A is the 2D area of the QW with the factor 2 accounting for the sum over spins, $I_{\mathrm{hm}}^{\mathrm{en}}$ is the overlap integral of the envelope functions of the nth and mth states in the CB and the VB, E_{cn} and E_{vm} are the energies of the nth and mth states in the CB and VB with kinetic energies $K_{\mathrm{c}}=\hbar^2k^2/2m_{\mathrm{e}}^*$ and $K_{\mathrm{v}}'=\hbar^2k'^2/2m_{\mathrm{h}}^*$, respectively, and f_{c} and f_{v} are the probability functions in their respective bands. For the sake of simplicity, we assume only electron and hole ground states are involved in the recombination process, so $\Sigma_{n,m}\rightarrow\Sigma_{0,0}$, where we assume $I_{\mathrm{h0}}^{\mathrm{e0}}=1$ and $\Sigma_{\vec{k},\vec{k}'}\delta_{\vec{k},\vec{k}'}=\Sigma_{\vec{k}}$ [19].

The total radiative recombination rate is then obtained from the summation over the photon energy spectrum spanned between the CB and VB ground states:

$$R_{\mathrm{tot,rad}}=\sum_{\omega}r_{\mathrm{d}}\left(E=\hbar\omega\right). \quad (2)$$

In figure 1, the radiative recombination time ($\tau=1/R_{\mathrm{tot,rad}}$) and the hole occupancy ($1-f_{\mathrm{v}}$) are displayed as a function of the hole concentration p_{v}; all material parameters are for a 12 nm long GaAs/$In_{0.2}Ga_{0.8}As$/GaAs QW [3]. It is seen that both quantities vary from exponential behavior for hole concentration $p_{\mathrm{v}}<10^{19}\mathrm{cm}^{-3}$ to saturation at unity and τ reaching $\cong 500$ ps, respectively, for $p_{\mathrm{v}}\geqslant 10^{19}\mathrm{cm}^{-3}$, in agreement with previous literature [20]. The saturation of hole occupancy $1-f_{\mathrm{v}}$ towards unity is caused by the Fermi level (E_{F}) crossing into the VB when the QW becomes degenerate at room temperature, which imposes a lower limit to the radiative recombination lifetime.

In figure 2(b), we compare the radiative recombination lifetime (purple curve) obtained from equation (2) with the Auger recombination lifetime (black curve) extracted from the experimental data in bulk $In_{0.53}Ga_{0.47}As$ [21], as a function of the average hole concentration in the QW. One can see that, for $p_0\geqslant 2\times10^{18}\mathrm{cm}^{-3}$, Auger scattering dominates the overall recombination process in the QW. In this comparison, we point out that the use of bulk values for experimental Auger recombination is realistic since for these high energy processes the effect of quantization if not negligible provides an upper bound to the carrier lifetime, as confinement generally increases the Coulomb interaction reducing the lifetime [22]. Consequently, the p_0 values for which Auger scattering dominates the overall recombination process is somehow overestimated.

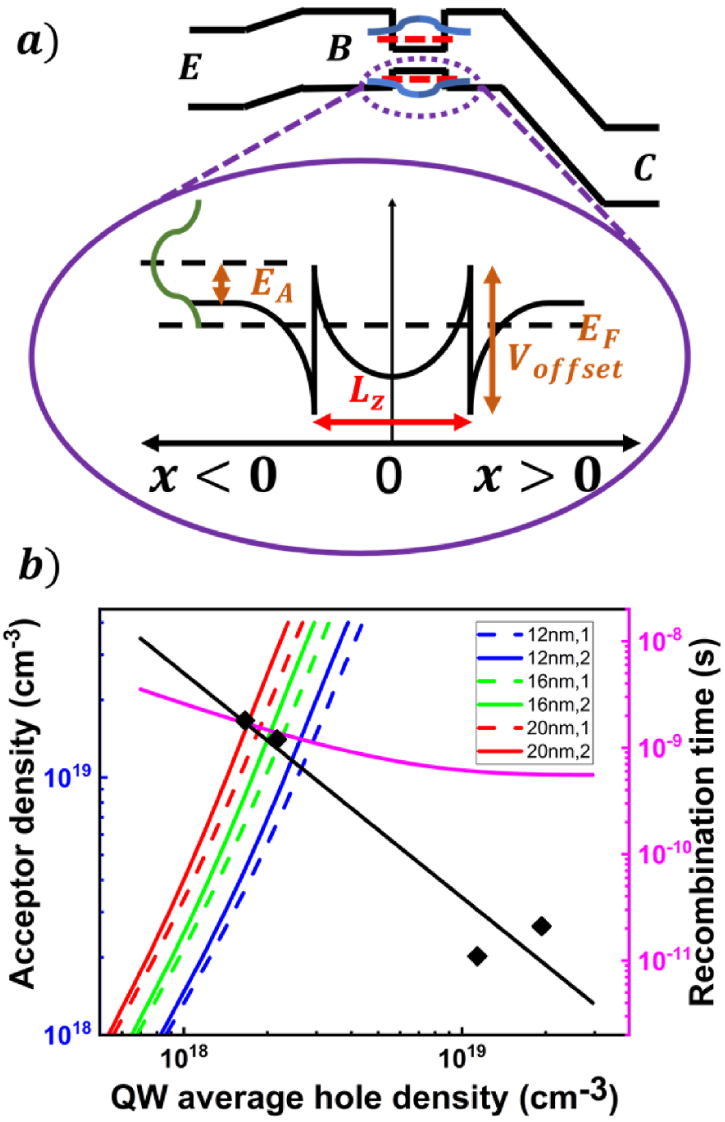

Figure 2. (a) Schematics of the TL band structure in normal active mode with E, B, and C designating the emitter, base and collector, respectively. The oval depicts the VB edge of the QW surrounded by a heavily p-doped base which contains a Gaussian density of state (DOS) for the impurity levels, indicated in dark green. All other symbols are defined in the text. (b) Comparison between radiative recombination times (purple curve) and experimental Auger recombination times (black dots numerically fitted in black line) [21] in the QW as a function of the average hole density. The relation between base acceptor density and hole density in the QW is shown for $\beta_A = 1$ (dashed lines) and $\beta_A = 2$ (solid lines), combined with different QW width $L_z = 12\,\text{nm}$ (blue curves), $L_z = 16\,\text{nm}$ (green curves) and $L_z = 20\,\text{nm}$ (red curves).

3. Hole concentration in the undoped QW

As the QW is undoped, we calculate self-consistently the average QW hole concentration as a function of the acceptor concentration N_A in the base by solving Poisson's equation:

$$\frac{d^2V}{dx^2} = \frac{e}{\epsilon}\left(N_A^-(V) - p^+(V)\right). \tag{3}$$

Here V is the self-consistent electrostatic potential, ϵ is the material dielectric constant, which we assume the same for GaAs and InGaAs, $N_A^-(V)$ is the concentration of ionized acceptors in the base region outside the QW, and $p^+(V)$ is the hole concentration across the base. We assume $N_A = 0$ in the QW of width L_z, and neglect the electron concentration that is much smaller than the majority carrier concentration, even during TL operation [6]. We also neglect the quantization in the VB of the QW, and treat the hole concentration classically, due to the weak confinement caused by the barrier, which mixes hole states in the QW with the

bulk base (see oval in figure 2(a)). Because of the heavy acceptor doping in the base, the acceptors form an impurity band, for which we assume a Gaussian DOSs [23, 24]:

$$g_{\mathrm{imp}}(E) = \frac{N_{\mathrm{A}}}{\sqrt{2\pi}\Delta E}\exp\left[-\frac{(E-E_{\mathrm{A}})^2}{2\Delta E^2}\right] \tag{4}$$

where N_{A} is the nominal acceptor concentration, E_{A} is the average binding energy of the impurity measured from the VB edge, assumed to be 19MeV [25] as the energy level of carbon-doped GaAs. ΔE is the broadening of the distribution obtained from the inter-ionic energy splitting [26] with the empirical equation $\Delta E = -1.52 + 1.74\times10^{-18}N_{\mathrm{A}} - 1.60\times10^{-38}N_{\mathrm{A}}^2$MeV for GaAs with doping density N_{A} varying from 10^{18} to $4\times10^{19}\mathrm{cm}^{-3}$. The hole DOS in the VB is given by:

$$g_{\mathrm{VB}} = \frac{1}{2\pi^2}\left(\frac{2m_{\mathrm{h}}^*}{\hbar^2}\right)^{\frac{3}{2}}\sqrt{E_{\mathrm{V}}-E} \tag{5}$$

where m_{h}^* is the heavy hole effective mass, and $E_V(V)$ is the potential dependent VB edge. We get:

$$N_{\mathrm{A}}^-(V) = \int_{-\infty}^{\infty}\frac{\mathrm{d}Eg_{\mathrm{imp}}(E+eV)}{1+\beta_{\mathrm{A}}\exp\dfrac{E-E_{\mathrm{F}}}{k_{\mathrm{B}}T}} \tag{6}$$

$$p^+(V) = \int_{-\infty}^{E_{\mathrm{v}}}\frac{\mathrm{d}Eg_{\mathrm{v.b.}}(E+eV)}{1+\exp\dfrac{E_{\mathrm{F}}-E}{k_{\mathrm{B}}T}} \tag{7}$$

where the factor β_{A} is the degeneracy factor in the occupation of the acceptor level, as derived by Landsberg [27].

Poisson's equation (equation (3)) is then solved for $p^+|_{x\to\pm\infty} = N_{\mathrm{A}}^-$ and by assuming the potential is symmetric around $x=0$ at the QW center, so that $\frac{\mathrm{d}V}{\mathrm{d}x}|_{x=0} = 0$. We also use the following boundary conditions i.e. $\frac{\mathrm{d}V}{\mathrm{d}x}|_{x=\pm\frac{L_z}{2}-} = \frac{\mathrm{d}V}{\mathrm{d}x}|_{x=\pm\frac{L_z}{2}+}$ and $V|_{x=\pm\frac{L_z}{2}+} = V|_{x=\pm\frac{L_z}{2}-} \mp V_{\mathrm{offset}}$ that express the continuity of the electric displacement (neglecting the difference between the dielectric constants of the InGaAs QW and the GaAs base), and the potential across the QW edges.

In figure 2(b), we display six curves relating the base acceptor density to the average hole density in the QW for three different QW widths $L_z = 12\,\mathrm{nm}$ (blue curves), $L_z = 16\,\mathrm{nm}$ (green curves) and $L_z = 20\,\mathrm{nm}$ (red curves) and two different acceptor degeneracy factors i.e. $\beta_{\mathrm{A}} = 1$ (solid curves) and $\beta_{\mathrm{A}} = 2$ (dashed curves) [27]. It is seen that as the QW width increases, the hole density decreases, which is due to the decreasing overlap between the hole concentrations leaking from both sides of the QW. Also, there is not much difference between both degeneracy factors; for instance, in a typical QW with $L_z = 12\,\mathrm{nm}$, a base doping density exceeding $5\times10^{18}\mathrm{cm}^{-3}$ provides a QW hole density larger than $2\times10^{18}\mathrm{cm}^{-3}$, which is the limit for the onset of Auger recombination, thereby, resulting in the poor TL quantum efficiency as the spontaneous radiative recombination lifetime saturates at ~0.5 ns. Therefore, lowering the base doping will quench Auger recombination, and increase the quantum efficiency, but will boost the QW carrier lifetime, detrimental to the speed performances.

4. Speed performance enhancement by engineering the TL turn-off time

The unique TL three-port design offers the opportunity to shorten the turn-off time by biasing the QW with an increasing reverse base-collector voltage V_{CB}, independently of the TL injection region, so that electrons escape quickly by field ionization, preventing recombination [28]. In figure 3(a), we schematically show the lasing mode of the QW, where the low n-doped collector depletion region is separated from the QW in the base region by a narrow heavily p-doped spacer of width x_{n}. Hence at $V_{\mathrm{CB}} = 0$ (on-mode), because of the large doping difference between p-base and n-collector, the depletion region extends almost exclusively deep into the collector with minimal extension into the base, thereby achieving flat-band condition around the QW. In order to assess the effect of quantum confinement of the spacer layer, we use the Transfer–Hamiltonian model [29, 30] to calculate the electron transition rate from the QW to the collector, as given by:

$$\frac{1}{\tau_{\mathrm{T}}} = \frac{2\pi}{\hbar}\sum_{\nu}|\langle\nu|-eFz|0\rangle|^2\delta(E_\nu - E_0) \tag{8}$$

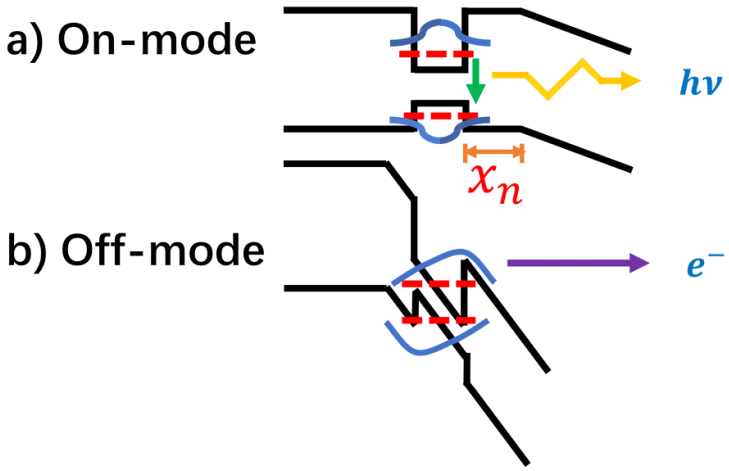

Figure 3. Schematic diagram illustrating the turn-off mechanism: (a) on-lasing state with TL base flat band; (b) off- lasing state with high reverse bias between the base and the collector, depleting the QW by field-emission tunneling.

Table 1. Parameters of the QW radiative recombination model.

Parameter	Value
m_e^*/m_0 (InGaAs)	0.058
m_h^*/m_0 (InGaAs)	0.48
E_g (eV) (InGaAs)	1.21
ϵ (GaAs/InGaAs)	$13.1\epsilon_0$
$\lvert\langle\hat{e}_0 \cdot P_{cv}\rangle\rvert^2/m_0$ (eV) (InGaAs)	3.53
V_{offset} (eV)	0.071
Temp (K)	300

Table 2. Transition time as a function of spacer thickness and the escape time.

Spacer x_n	On-mode transition time	Off-mode escape time
5 nm	0.69 ns	0.17 ps
10 nm	0.34 μs	0.17 ps
15 nm	162 μs	0.17 ps

where $|0\rangle$ is the initial state in the base (QW and spacer combined), $|\nu\rangle$ is the final state in the collector, $F = 2.4 \times 10^5 \mathrm{V\,cm^{-1}}$ is the built-in field of the base-collector junction [3] and τ_T is the transition time. In table 1, the transition time shows an exponential increase as the spacer widens. Hence, for $x_n \geqslant 10$ nm, one gets $1/\tau_T \ll R_{tot,rad} < R_{tot}$ so that electrons cannot escape by tunneling before recombining [31, 32].

In figure 3(b), we display the schematic of the band diagram for the off-lasing mode set by quickly reverse-biasing V_{CB}, in order to deplete the x_n region to extend the built-in field of the base-collector junction slightly beyond the QW to cause the electrons to leak by tunneling across the triangular barrier. In this context, the collector-base voltage (V_{CB}) needed for a depleting the QW reads:

$$V_{CB} = V_{QW} + V_{x_n} + V_{collector} \tag{9}$$

where we ignore voltage drops in high-doping regions outside the base-collector junction. Here $V_{collector}$ and V_{x_n} are the voltage drops across the depleted collector region and the spacer, respectively, and V_{QW} is the bias across the QW to field ionize the electrons and turn lasing off. If one assumes V_{QW} corresponds to half of the CB offset (~104 meV), the average field in the QW is $F_{off} = 4.3 \times 10^4 \mathrm{V\,cm^{-1}}$. By directly solving Schrödinger equation for a QW in a constant electric field, one obtains the escape time [33]:

$$\tau_{escape} = \hbar/\Gamma \tag{10}$$

where Γ is the resonant decay width for the triangular tunneling barrier. In table 2, we display the escape time for a QW width [3] $L_Z = 12$ nm, which is ~0.2ps (independent of the spacer), which is much faster than the recombination time and consistent with our group's previous work [34].

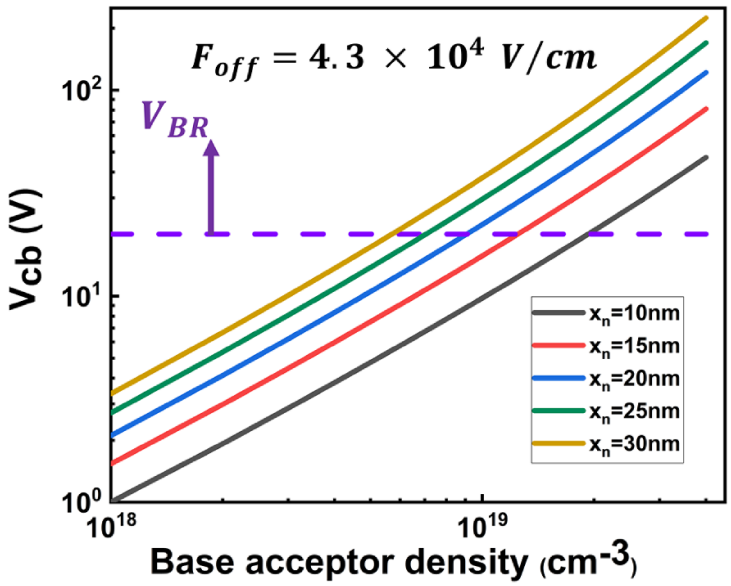

Figure 4. Reverse bias for depleting the QW to turn off stimulated emission as a function of the acceptor density in the base region, and for four different spacers x_n between the QW and the collector region. The dashed purple line indicates the limit for breakdown.

In figure 4, solutions of Poisson's equation in the depletion approximation show the base-collector voltage required to field-ionize a 12 nm wide InGaAs QW as a function of the bases p-doping density for different x_n spacers. The overall excess electric field for lasing turn-off therefore consists of F_{off} augmented by the field (F_A) to deplete the p-doped x_n spacer:

$$F_A = \frac{e}{\epsilon}\int_0^{x_n} N_A^- \, dx = \frac{e}{\epsilon} N_A \times x_n \tag{11}$$

where N_A^- is the density of ionized acceptors, which we approximate as N_A (the acceptor density in the base region).

Figure 4 indicates that lower thickness and lighter doping density will result in a smaller V_{CB}, as expected. Encouragingly, V_{CB} can be reduced to a few volts when base p-doping is reduced to $N_A \sim 10^{18}\text{cm}^{-3}$, which is more than one order of magnitude less than the actual TL base doping, therefore limiting considerably Auger losses for improved quantum efficiency. We also indicate the value of the avalanche breakdown voltage of 20 V for the n-GaAs ($N_D < 10^{17}\text{cm}^{-3}$) [35] collector, which will be detrimental to the turn-off process, and is consequently the upper limit to V_{CB}.

5. Conclusions

In summary, the TL three-terminal design enables a new turn-off lasing mechanism by reverse biasing the base-collector voltage to remove electrons from the QW by tunneling through the confining potential barrier, thereby precluding recombination with holes, and enhancing the TL speed response. In addition, we showed that proper adjustment of base doping concentration and base inter-layer thickness will prevent base-collector breakdown. The low doping requirement for turn-off mechanism anticipates a significant improvement of the TL performances by quenching Auger recombination.

Data availability statement

The data that support the findings of this study are available upon reasonable request from the authors.

Acknowledgments

This work is sponsored in part by E2CDA-NRI, a funded center of NRI, a Semiconductor Research Corporation (SRC) program sponsored by NERC and NIST under Grant No. NERC 2016-NE-2697-A and by the National Science Foundation under Grant No. ECCS 16-40196.

ORCID iD

Bohao Wu https://orcid.org/0000-0003-0128-8459

References

[1] Feng M, Holonyak N and Chan R 2004 *Appl. Phys. Lett.* **84** 1952
[2] Walter G, Holonyak N, Feng M and Chan R 2004 *Appl. Phys. Lett.* **85** 4768
[3] Feng M, Holonyak N, Walter G and Chan R 2005 *Appl. Phys. Lett.* **87** 131103
[4] Walter G, Wu C H, Then H W, Feng M and Holonyak N 2009 *Appl. Phys. Lett.* **94** 231125
[5] Then H W, Feng M and Holonyak N 2010 *J. Appl. Phys.* **107** 094509
[6] Then H W, Feng M and Holonyak N 2013 *Proc. IEEE* **101** 2271
[7] Winoto A, Qiu J, Wu D and Feng M 2019 *IEEE Nanotechnol. Mag.* **13** 27
[8] Zhang L and Leburton J P 2009 *IEEE J. Quantum Electron.* **45** 359
[9] Faraji B, Shi W, Pulfrey D L and Chrostowski L 2009 *IEEE J. Sel. Top. Quantum Electron.* **15** 594
[10] Shirao M, Lee S, Nishiyama N and Arai S 2011 *IEEE J. Quantum Electron.* **47** 359
[11] Basu R, Mukhopadhyay B and Basu P K 2011 *Semicond. Sci. Technol.* **26** 105014
[12] Taghavi I, Kaatuzian H and Leburton J P 2012 *Appl. Phys. Lett.* **100** 231114
[13] Taghavi I, Kaatuzian H and Leburton J P 2013 *IEEE J. Quantum Electron.* **49** 426
[14] Li Y and Leburton J P 2018 *Appl. Phys. Lett.* **113** 171110
[15] Hsieh C T and Chang S W 2019 *IEEE J. Sel. Top. Quantum Electron.* **25** 1501508
[16] Li Y and Leburton J P 2019 *J. Appl. Phys.* **126** 153103
[17] Schnitzer I, Yablonovitch E, Caneau C, Gmitter T J and Scherer A 1993 *Appl. Phys. Lett.* **63** 2174
[18] Chuang S L 2012 *Physics of Photonic Devices* vol 126 (New York: Wiley) pp 347–75
[19] This is an overestimate of the radiative rate as the overlap between CB and VB states is generally smaller than unity, because of the leaking of the VB wave function into the GaAs barrier (see the discussion of equation 3)
[20] Bhattacharya P and Pang L Y 1994 *Phys. Today* **47** 64
[21] Ahrenkiel R K, Ellingson R, Johnston S and Wanlass M 1998 *Appl. Phys. Lett.* **72** 3470
[22] Wang J and Leburton J P 1994 *IEEE Photonics Technol. Lett.* **6** 1091
[23] Lucovsky G 1965 *Solid State Commun.* **3.5** 105
[24] Taylor G W, Chatterjee P K and Chao H H 1980 *IEEE Trans. Electron Devices* **27** 199
[25] Sze S M and Irvin J C 1968 *Solid State Electron.* **11** 599
[26] Lukes T, Nix B and Suprapto B 1972 *Phil. Mag.* **26** 1239
[27] Landsberg P T 1969 *Solid-State Theory: Methods and Applications* (New York: Wiley/Interscience) p 266
[28] This mechanism is different from the TL modulation by photon-assisted tunneling (Franz–Keldysh effect) that takes place all over the depletion region of the base-collector junction (see e.g. Wu M K, Feng M and Holonyak N 2012 *Appl. Phys. Lett.* **101** 081102)
[29] Duke C B 1969 Tunneling in solids vol 10 (New York: Academic) p 210
[30] Leburton J P, Kolodzey J and Briggs S 1988 *Appl. Phys. Lett.* **52** 1608
[31] Feng M, Holonyak N Jr, James A, Cimino K, Walter G and Chan R 2006 *Appl. Phys. Lett.* **89** 113504
[32] Then H W, Walter G, Feng M and Holonyak N Jr 2008 *Appl. Phys. Lett.* **93** 163504
[33] Panda S and Panda B K 2001 *Pramana* **56** 809
[34] Wang J, Leburton J P, Educato J and Zucker J 1993 *J. Appl. Phys.* **73** 4669
[35] Sze S M and Gibbons G 1966 *Appl. Phys. Lett.* **8** 111